ARFs 1 and 3 were separated on a gradient of decreasing $(NH_4)_2SO_4$ concentration.

28. G. M. H. Thomas *et al.*, *Cell* **74**, 919 (1993).
29. The nonconserved NH_2-termini of ARF proteins are chemically blocked by acylation. The solid underlined peak 1 peptide sequence was found in two discrete high-performance liquid chromatography (HPLC) fractions. The absence of phenylhydantoin (PTH)-valine at position 16 of this peptide (*) in Fig. 2 identified peak 1 as either the type I or III isoform. Time of flight mass analysis of the two HPLC fractions performed on a Finnigan Lasermat with an α-cyano-4-hydroxycynammic acid matrix gave values of 2047 and 2064 D, corresponding to the type I or III peptide containing unoxidized and oxidized methionine residues, respectively.
30. Sequence corresponding to full-length ARF1 was amplified from a rat brain cDNA library with specific oligonucleotides. Polymerase chain reaction (PCR) primers were designed with Nde I and Bgl II restriction sites to facilitate cloning of the amplified cDNA fragments into the pET3C expression vector. Several of the cloned PCR fragments were sequenced with the T7 Sequensing system (Pharmacia) to prove the identity of the amplified products. BL21 (DE3) cells were transformed with pET3C-ARF construct and expression of recombinant ARF1 was induced with isopropylthio-β-galactoside at a final concentration of 0.4 mM. Two hours after induction, bacterial cells were collected by centrifugation. Purification of the recombinant protein was done as described (*11*) except that gel filtration (Superdex 75) was done in PIPES buffer. Purity was assessed by SDS-PAGE. Samples obtained after gel filtration were concentrated and used directly. GTP-γ-S binding to ARF was assessed as described (*11*).
31. We thank the Wellcome Trust and the Royal Society for their support. A.F. and E.C. were supported by studentships from Yamanouchi and SERC, respectively.

22 November 1993; accepted 14 December 1993

Maspin, a Serpin with Tumor-Suppressing Activity in Human Mammary Epithelial Cells

Zhiqiang Zou, Anthony Anisowicz, Mary J. C. Hendrix,* Ann Thor, Mark Neveu,† Shijie Sheng, Kristina Rafidi, Elisabeth Seftor,* Ruth Sager‡

A gene encoding a protein related to the serpin family of protease inhibitors was identified as a candidate tumor suppressor gene that may play a role in human breast cancer. The gene product, called maspin, is expressed in normal mammary epithelial cells but not in most mammary carcinoma cell lines. Transfection of MDA-MB-435 mammary carcinoma cells with the maspin gene did not alter the cells' growth properties in vitro, but reduced the cells' ability to induce tumors and metastasize in nude mice and to invade through a basement membrane matrix in vitro. Analysis of human breast cancer specimens revealed that loss of maspin expression occurred most frequently in advanced cancers. These results support the hypothesis that maspin functions as a tumor suppressor.

We have used subtractive hybridization (*1–5*) and the "differential display" method (*6, 7*) to identify candidate tumor suppressor genes that are defective in human breast carcinoma cells. These genes, now totaling more than 30, were identified initially by searching for mRNAs whose expression is reduced or absent in tumor cells compared with normal cells grown under similar conditions.

One of the genes we have identified by this approach encodes a member of the serpin family of protease inhibitors, which we have termed "maspin." A single 3.0-kb maspin mRNA is expressed in normal mammary epithelial cell strains (*8*), but not in most mammary tumor cell lines examined (those shown in Fig. 1, as well as MDA-MB-157, MDA-MB-231, MDA-MB-436, MDA-MB-468, BT-549, and Hs 578T cells) nor in foreskin- or breast-derived fibroblasts (*9*). Southern (DNA) blot analysis (*9*) of Xba I–restricted DNA from normal and tumor cells with a maspin complementary DNA (cDNA) probe revealed no gross structural alterations of the maspin gene in the tumor cells. This result suggests that the maspin gene is downregulated but not mutated in cancer cells.

Maspin cDNA was isolated from a library prepared from normal human mammary epithelial (76N) cells. The cDNA sequence contains 2584 nucleotides, including 75 nucleotides of 5′ and 1381 nucleotides of 3′ untranslated sequence. It encodes a protein of 375 amino acids, with an NH_2-terminal methionine and COOH-terminal valine, and eight internal cysteine residues that may form two or more disulfide bonds to stabilize the protein's tertiary structure (Fig. 2A). The initiation codon and surrounding nucleotides fit the Kozak consensus (*10*).

Maspin displays significant sequence similarity to the serpin superfamily of serine protease inhibitors (Fig. 2B), with highest amino acid identity to the equine and human neutrophil-monocyte elastase inhibitors (43% and 39%, respectively), human

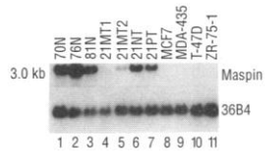

Fig. 1. Northern (RNA) blot analysis of maspin mRNA in normal and tumor cells. Total cellular RNA was isolated from exponentially growing cells cultured in DFCI-1 medium (*8*). Total RNA (20 μg of RNA per lane) was subjected to electrophoresis on a 1% formaldehyde-agarose gel, transferred to nylon membrane, and hybridized with a ^{32}P-labeled maspin probe. Lanes labeled 70N, 76N, and 81N contain RNA from normal breast epithelial cells; all other lanes contain RNA from breast tumor cells. 21NT and 21PT are primary tumor lines; 36B4 is a loading control (*5*).

Table 1. Tumorigenicity of maspin-transfected MDA-MB-435 cells. Cells (5×10^5) were resuspended in phosphate-buffered saline and injected into the mammary fat pads of nude mice. Each mouse was injected at two sites. In one experiment, the mice were 8 to 10 weeks old when injected; in the second, they were 4 to 6 weeks old. Tumor development was monitored weekly. Numbers in parentheses are the numbers of tumors at 10 weeks after injection. The number of tumors is smaller at 10 weeks than at 6 weeks because some animals died. CA, carcinoma; ND, not done; NT, no tumor. $P = 0.034$ for mice T1 through T6; $P = 0.00057$ for mice T4 through T6 (Student's one-sided t test).

Cells	Tumors/sites injected at 6 weeks	Mean tumor weight at 10 weeks (g)	Metastases	
			Lung	Lymph nodes
pCMVneo N1	8/10	0.74 (7)	CA	CA
pCMVneo N2	10/10	1.77 (6)	CA	CA
pCMVmaspin T1	8/10	1.67 (4)	ND	ND
pCMVmaspin T4	6/10	0.31 (7)	NT	NT
pCMVmaspin T5	5/10	0.35 (7)	NT	NT
pCMVmaspin T6	8/10	0.43 (9)	NT	NT

Z. Zou, A. Anisowicz, M. Neveu, S. Sheng, K. Rafidi, R. Sager, Division of Cancer Genetics, Dana-Farber Cancer Institute, 44 Binney Street, Boston, MA 02115.
M. J. C. Hendrix and E. Seftor, University of Arizona Cancer Center, Tucson, AZ 85724.
A. Thor, Department of Pathology, Massachusetts General Hospital, 100 Blossom Street, Boston, MA 02114.

*Present address: Pediatric Research Institute, 3662 Park Avenue, St. Louis, MO 63110.
†Present address: Pfizer Central Research Building, Groton, CT 06340.
‡To whom correspondence should be addressed.

plasminogen activator inhibitor type 2 (PAI-2; 31%), human squamous cell carcinoma antigen (34%), and chicken ovalbumin (31%). Active serpins (S-form) interact with their target proteases with 1:1 stoichiometry to form stable, denaturation-resistant complexes in which the protease is inactive. The P_1 residue located NH_2-terminal to the reactive center plays an important role in determining target specificity. Serpins with Ala, Val, or Met inhibit elastase-like proteinases, whereas serpins with Arg at the P_1 position inhibit trypsin-like proteases (*11*, *12*). Maspin appears to be an Arg serpin, as judged from the sequence comparisons (Fig. 2B).

Peptides corresponding to three poorly conserved sequences in maspin were synthesized and conjugated to keyhole limpet hemocyanin (*13*) for polyclonal antibody production. Three antibodies, designated AbS1A, AbS3A, and AbS4A, were studied (Fig. 2B). AbS4A recognizes the reactive center loop encompassing the putative P_1-P_1' residues. All three antibodies reacted with a 42-kD protein present in normal cells (70N) and in tumor cells (MDA-435) transfected with maspin cDNA. In contrast, there was no reactive protein in tumor cell lines or in *neo*-transfected controls (Fig. 2C).

Mammary carcinoma cell line MDA-MB-435 forms tumors at the site of orthotopic injection and metastasizes in nude mice (*14*). To investigate whether maspin affected tumor formation in nude mice, we transfected MDA-MB-435 cells with a vector containing the maspin gene under the control of the cytomegalovirus (CMV) promoter (*5*). The maspin-transfected cells expressed a 2.0-kb mRNA and 42-kD protein at levels similar to those seen in normal cells, whereas the *neo* controls expressed no maspin gene products (*9*).

Four maspin transfectants and two *neo* controls were further tested by injection into nude mice (*14*, *15*) (Table 1). Three of the four maspin transfectant clones produced much smaller tumors than the vector controls, whereas one clone (T1) produced tumors like those of MDA-MB-435 and the *neo* controls. Histopathological examination of the lungs and lymph nodes revealed differences between the two controls and the three transfectants (T4, T5, and T6). No tumors were seen in lung or lymph

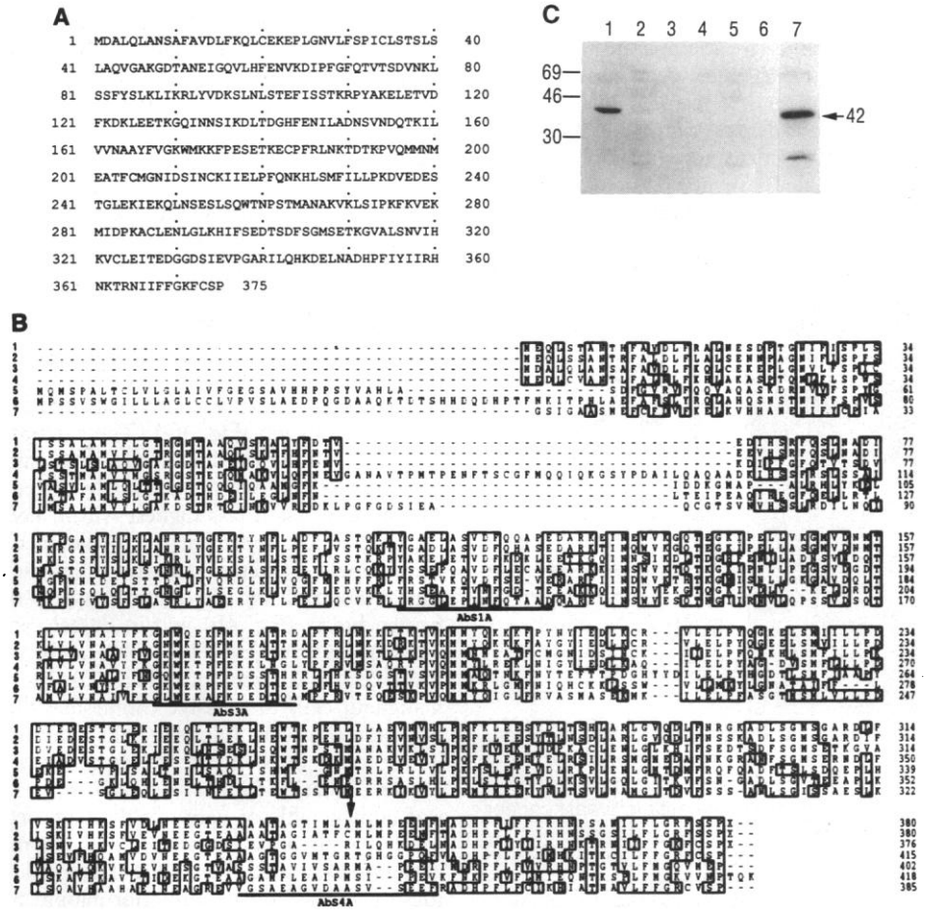

Fig. 2. (**A**) Predicted amino acid sequence of maspin (*22*). Complementary DNA sequencing was performed with an ABI 373A automated DNA sequencer at the core facility of the Dana-Farber Cancer Institute. The nucleotide sequence has been deposited in GenBank (accession number U04313). (**B**) Comparison of the maspin amino acid sequence with those of other serpins. Identical residues are boxed. Three regions used for antibody production are underlined. The arrow denotes the proposed reactive center of maspin. Row 1, horse serapin; row 2, human monocyte-neutrophil elastase inhibitor; row 3, maspin; row 4, human plasminogen activator inhibitor type 2; row 5, human plasminogen activator inhibitor type 1; row 6, α_1-antitrypsin; row 7, ovalbumin. (**C**) Detection of maspin protein from normal and tumor cells by immunoblotting. Cells were lysed in electrophoresis sample buffer, and the extracts were subjected to electrophoresis on a 10% SDS-polyacrylamide gel and transferred to Immobilon membrane. Maspin was detected by antibody AbS1A with the ECL (enhanced chemiluminescence) system (Amersham). Lane 1, 76N cells; lanes 2 to 5, tumor cells MCF7, MDA-MB-468, MDA-MB-435, and ZR-75-1, respectively; lane 6, MDA-MB-435 *neo* transfectant; and lane 7, MDA-MB-435 maspin transfectant. Size markers are indicated in kilodaltons.

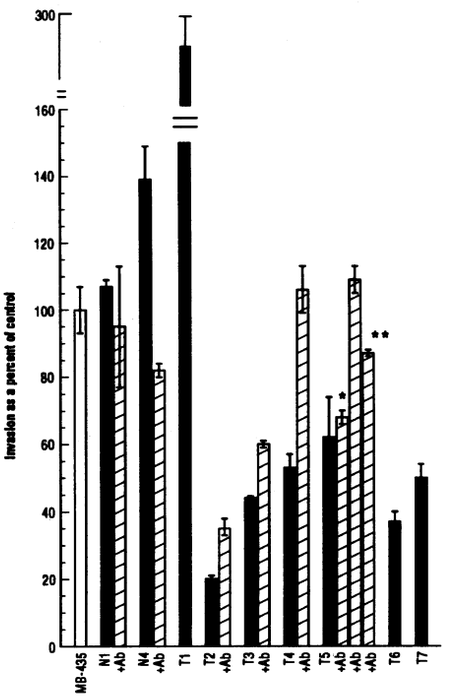

Fig. 3. Effect of maspin transfection on invasive potential in vitro of MDA-MB-435 cells (*23*). The invasion data from the nontransfected MDA-MB-435 cells were normalized to 100%, and the invasion data from the maspin and *neo* transfectants are expressed as a percentage of this control. The data represent the average of two separate experiments, and the error bars represent the standard error of the mean and are based on $n = 6$ for each experiment. To neutralize the activity of secreted maspin, we pretreated selected clones with AbS4A (+Ab) (1.0 μg/ml) continuously during the course of the invasion assay. In some experiments, AbS4A was tested at 0.1 μg/ml (single asterisk) and 3.0 μg/ml (double asterisks). The invasion data from the untreated cells were normalized to 100%, and, as above, the invasion data from the treated cells are expressed as a percentage of these controls.

nodes from the mice injected with the maspin transfectants, whereas the *neo* controls produced neoplastic pleural effusions and multifocal, pulmonary parenchymal metastatic carcinoma. Additional tumor masses were present in central venous blood vessels, the diaphragm, and lymph nodes. The lymph node specimens from these control mice contained carcinoma in some samples and medullary mesenchymal cell hyperplasia in others. These results, though preliminary (only two mice were examined from each cell line tested), suggest that maspin expression leads to decreased growth and metastasis of tumor cells in vivo. In contrast, in cell culture, the maspin transfectants, the *neo* controls, and the parental MDA-MB-435 cells grew at similar rates (9), which suggests that the inhibition seen in the mice was not simply the result of an intrinsic growth defect in the maspin transfectants.

We also used an in vitro assay of tumor cell invasion through reconstituted basement membrane (Matrigel) to assess the functional activity of maspin (*16*) (Fig. 3). Seven maspin-transfectant clones and two *neo*-transfectant clones were compared with the parental MDA-MB-435 cells. Six of the seven maspin transfectants (clones T2 to T7) showed reduced invasive ability; this ability was restored in a dose-dependent manner by addition of affinity-purified AbS4A. The exceptional clone (T1), which also failed to inhibit tumor growth in nude mice (Table 1), may have undergone an additional genetic change or changes. Immunostaining of T4 transfectants after invasion through Matrigel revealed that 95% of the invading cells were maspin-negative. The two *neo* controls resembled the parental MDA-MB-435 cells in invasive activity. We have recently found that addition of purified recombinant maspin in nanomolar concentrations inhibits the invasive capacity of tumor cells in this assay (*17*).

Liotta and Stetler-Stevenson's model for tumor cell invasion (*18*) postulates that tumor cells must adhere to the extracellular matrix, degrade it, and migrate through it. We found no significant differences in the ability of the maspin transfectants and control cells to adhere to Matrigel. Cinematography studies of cell motility, on the other hand, revealed a significant decrease in the motility of the transfectants compared with that of controls (*19*), which corroborates the invasion results (Fig. 3).

Indirect immunofluorescence microscopy of normal human mammary epithelial (76N) cells demonstrated that maspin is localized mainly in the pericellular space, although small amounts are present in the cytoplasm (Fig. 4A). These results suggest that maspin is secreted into the extracellular matrix and may interact with its target protease there or on the plasma membrane. AbS1A, AbS3A, and AbS4A all generated similar staining patterns that could be eliminated by preabsorption with the corresponding immunizing peptide. Acetone-fixed cryosections and formalin-fixed, paraffin-embedded sections of benign breast tissues (n = 6) and benign epithelium adjacent to invasive carcinomas were positive for maspin when immunostained with AbS4A. Maspin expression was particularly intense in myoepithelial cells, both within large ducts and within terminal duct lobular units. Luminal epithelial cells were heterogeneously positive (with some cells showing weak granular cytoplasmic immunoreactivity), with more intense apical reactivity and some reactivity of intraluminal secreted material (Fig. 4B). Inflammatory and stromal cells were always negative.

Twelve invasive human breast carcinomas, eleven regional lymph node metastases, two pleural effusions containing metastatic breast cancer, and adjacent in situ epithelial elements were also evaluated for maspin expression (Fig. 4G). The carcinoma in situ was weakly immunopositive, and apical reactivity was occasionally noted. Maspin expression was highest within myoepithelial cells (adjacent to the basement membrane). Secreted maspin was sometimes observed in the luminal space of benign breast (Fig. 4B) and in ductal carcinomas in situ (Fig. 4C), but rarely in invasive ductal carcinomas (Fig. 4D). Most malignant cells in invasive carcinomas did not express maspin (Fig. 4E), but a minority of cells in well-differentiated tumors expressed maspin focally (Fig. 4G). Maspin was undetectable or very weakly expressed in all lymph node metastases and pleural effusions examined (Fig. 4F). These findings suggest a biological role for maspin in benign breast tissue and a potentially pivotal alteration in maspin expression during the progression of breast cancer.

Several lines of evidence presented here support the hypothesis that maspin functions as a class II tumor suppressor gene in human breast epithelial cells (*2*, *7*). It is noteworthy that maspin down-regulation in tumor cell lines is consistent with the loss of maspin expression in tumor tissues. Although other serpins, especially PAI-1 and PAI-2, have been implicated indirectly in the inhibition of tumor cell invasion by

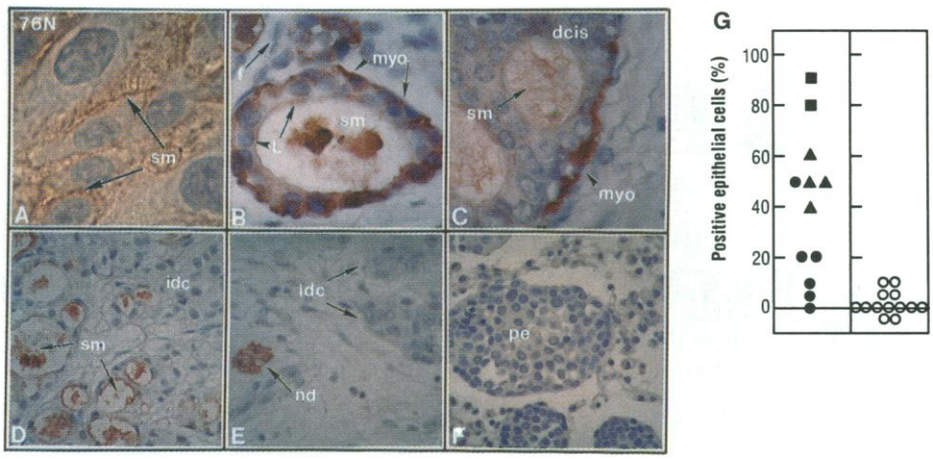

Fig. 4. Immunoperoxidase staining of maspin in cultures of acetone-fixed normal mammary epithelial cells (**A**) and in formalin-fixed, paraffin-embedded sections of benign (**B**) and cancerous (**C** to **F**) breast tissue. In (C) is shown a ductal carcinoma in situ; invasive ductal carcinomas are shown in (D) and (E); and a pleural effusion containing metastatic breast cancer is shown in (F). Maspin immunoreactive sites were unmasked in formalin-fixed sections by pretreatment of the sections in 10% sucrose at 80°C for 2 hours. Both cell cultures and tissue sections were incubated with AbS4A (5 μg/ml) before immunoperoxidase detection with biotinylated tyramine (*24*). 3-Amino-9-ethylcarbazole was used as the chromagen, and nuclei were counterstained with Mayer's hematoxylin. Preabsorption of the AbS4A with immunizing peptide eliminated all specific maspin staining. Abbreviations: Sm, secreted maspin; L, luminal cell; myo, myoepithelial cell; f, fibroblast; dcis, ductal carcinoma in situ; idc, invasive ductal carcinoma; nd, normal benign breast duct; pe, pleural effusion. (**G**) Reactivity of AbS4A with human breast carcinomas. Affinity-purified AbS4A (5 μg/ml) was reacted with formalin-fixed, paraffin-embedded sections that were pretreated in 10% sucrose at 80°C for 1 hour. Immune complexes were visualized by a modified immunoperoxidase method with biotinylated tyramine (*24*). The percentage of positive cells denotes the number of carcinoma cells that were reactive with AbS4A divided by the total number of tumor cells (×100) in primary breast carcinomas (left) and mammary lymph node metastases and pleural effusions (right). Each symbol represents a specimen from a different individual. Many tumor cells in ductal carcinomas in situ (■) expressed maspin. Differentiated components of invasive breast carcinomas (▲) expressed an intermediate amount of maspin, whereas many poorly differentiated neoplasms (●), lymph node metastases, and pleural effusions (○) expressed little or no maspin.

virtue of their known activity against plasminogen activators, their role as tumor suppressors in breast cancer is not established (*20*). Similarly, the activity of metalloproteinase inhibitors in breast cancer is not yet known (*21*).

From a clinical perspective, maspin offers substantial opportunities. First, the loss of expression that occurs during malignant progression of primary tumors suggests that maspin has potential value as a marker of a favorable prognosis. Maspin may also have therapeutic potential. The maspin gene is not lost in tumor cells but rather is down-regulated, as shown by the partial loss of expression in primary carcinomas and by its up-regulation in tumor cells after treatment with a phorbol ester (*9*). Maspin offers the potential of novel pharmacological approaches to therapy, such as inducing re-expression of the protein in breast cancers or blocking expression of the target protease.

REFERENCES AND NOTES

1. R. Sager, *Science* **246**, 1406 (1989).
2. S. W. Lee, C. Tomasetto, R. Sager, *Proc. Natl. Acad. Sci. U.S.A.* **88**, 2825 (1991).
3. S. W. Lee, C. Tomasetto, K. Swisshelm, K. Keyomarsi, R. Sager, *ibid.* **89**, 2504 (1992).
4. S. Lee, C. Tomasetto, D. Paul, K. Keyomarsi, R. Sager, *J. Cell Biol.* **118**, 1213 (1992).
5. C. Tomasetto, M. S. Neveu, J. Daley, P. K. Horan, R. Sager, *ibid.* **122**, 157 (1993).
6. P. Liang, L. Averboukh, K. Keyomarsi, R. Sager, A. B. Pardee, *Cancer Res.* **52**, 6966 (1992).
7. R. Sager, A. Anisowicz, M. Neveu, P. Liang, G. Sotiropoulou, *FASEB J.* **7**, 964 (1993).
8. V. Band and R. Sager, *Proc. Natl. Acad. Sci. U.S.A.* **86**, 1249 (1989).
9. Z. Zou *et al.*, unpublished observations.
10. M. Kozak, *Nucleic Acids Res.* **12**, 857 (1984).
11. J. Travis, A. Guzdek, J. Potempa, W. Watorek, *Biol. Chem. Hoppe Seyler* **371**, 3 (1990).
12. R. Huber and R. W. Carrell, *Biochemistry* **28**, 8951 (1989).
13. E. Harlow and D. Lane, in *Antibodies: A Laboratory Manual* (Cold Spring Harbor Laboratory, Cold Spring Harbor, NY, 1988), chap. 8.
14. J. E. Price, A. Polyzos, R. D. Zhang, L. M. Daniels, *Cancer Res.* **50**, 717 (1990).
15. At 10 weeks after inoculation, all mice were killed and their tumors excised and weighed. Lymph nodes adjacent to the site of injection and lungs were also removed and preserved for histological examination. Multiple 5-μm sections of lung and lymph nodes from each animal were stained with hematoxylin and eosin. Specimens were coded, and their identity was unknown to the pathologist.
16. M. J. C. Hendrix, E. A. Seftor, R. E. B. Seftor, I. J. Fidler, *Cancer Lett.* **38**, 137 (1987).
17. S. Sheng and R. Sager, unpublished observations.
18. L. Liotta and W. G. Stetler-Stevenson, *Cancer Res.* **51**, 5054 (1991).
19. M. J. C. Hendrix, unpublished observations.
20. J. E. Testa and J. P. Quigley, *Cancer Metastasis Rev.* **9**, 353 (1990).
21. W. G. Stetler-Stevenson, S. Aznavoorian, L. A. Liotta, *Annu. Rev. Cell Biol.* **9**, 541 (1993).
22. Abbreviations for the amino acid residues are A, Ala; C, Cys; D, Asp; E, Glu; F, Phe; G, Gly; H, His; I, Ile; K, Lys; L, Leu; M, Met; N, Asn; P, Pro; Q, Gln; R, Arg; S, Ser; T, Thr; V, Val; W, Trp; and Y, Tyr.
23. The ability of maspin-transfected clones (T1 to T7) to penetrate Matrigel-coated (Becton Dickinson, Boston, MA) polycarbonate filters (containing 10-μm pores) was measured with the membrane invasion culture system (MICS) (*16*). Cells (1×10^5) were seeded into the upper wells of the MICS chamber onto the Matrigel-coated filter in Dulbecco's minimum essential medium containing 10% NuSerum (Becton Dickinson). After 72 hours of incubation at 37°C with constant O_2 and CO_2 exchange, the cells that invaded the filter were collected, stained, and counted.
24. J. C. Adams, *J. Histochem. Cytochem.* **40**, 1457 (1992).
25. We thank P. Pemberton for advice on serpin structure; H. B. Warren for histopathologic examination of animal tissues; A. B. Pardee, B. Zetter, and C. Li for helpful suggestions; K. Ryan for technical assistance; and M. Connolly for preparing the manuscript. Supported by NIH grants to R.S. (PO1 CA22427 and OIG CA39814) and to M.J.C.H. (RO1 CA59702). M.N. was a recipient of an Interdisciplinary Program in Health Fellowship from the Harvard School of Public Health.

2 November 1993; accepted 15 December 1993

Visualization of Quantal Synaptic Transmission by Dendritic Calcium Imaging

Timothy H. Murphy,* Jay M. Baraban, W. Gil Wier, Lothar A. Blatter†

As changes in synaptic strength are thought to be critical for learning and memory, it would be useful to monitor the activity of individual identified synapses on mammalian central neurons. Calcium imaging of cortical neurons grown in primary culture was used to visualize the activation of individual postsynaptic elements by miniature excitatory synaptic currents elicited by spontaneous quantal release. This approach revealed that the probability of spontaneous activity differed among synapses on the same dendrite. Furthermore, synapses that undergo changes in activity induced by glutamate or phorbol ester treatment were identified.

Miniature excitatory synaptic currents (MESCs) are a fundamental form of neuronal communication produced by the spontaneous release of a single transmitter quantum (*1*). Experiments suggest that at central synapses a single MESC is equivalent to a postsynaptic response resulting from the evoked activation of a single synaptic terminal (*2*). By analogy with quantal analysis used to define mechanisms of synaptic plasticity at neuromuscular junctions, analysis of MESCs has been used to provide information about changes in release probability and postsynaptic responsiveness in models of plasticity in brain neurons (*1*). Prompted by concerns that assumptions implicit in these analyses may not be applicable to populations of central synapses (*3*), we have visualized postsynaptic calcium transients induced by MESCs to monitor activity at individual synapses.

For this approach we used rat cerebral cortical neurons grown in primary culture (*4*, *5*) because they form functional synapses and exhibit synaptically induced free cytoplasmic Ca^{2+} $[Ca^{2+}]_i$ transients in postsynaptic dendritic processes detectable in neurons microinjected with the Ca^{2+}-sensitive probe fura 2 (*6*–*8*). In the presence of tetrodotoxin (TTX) and the absence of extracellular Mg^{2+} (*4*), highly localized $[Ca^{2+}]_i$ transients, which we termed miniature synaptic calcium transients (MSCTs), were observed in spiny distal dendritic segments (Fig. 1). The MSCTs arose from an initial focal point of 1 to 2 μm^2 and spread along the dendritic axis to produce a $[Ca^{2+}]_i$ elevation that extended ~10 μm. The distance between synaptic terminals aligned on a dendrite and labeled with synaptophysin or rhodamine 123 was estimated to be 2.3 ± 0.7 and 2.7 ± 0.9 μm (mean ± SD), respectively (*9*). Thus, the highly localized initiation of the MSCTs likely reflects spontaneous quantal release from a single presynaptic terminal and the subsequent $[Ca^{2+}]_i$ transient in the postsynaptic dendrite.

MSCTs appeared to be mediated by activation of *N*-methyl-D-aspartate (NMDA) receptors by released glutamate (Glu), because in the presence of the competitive antagonist DL-2-amino-5-phosphonovaleric acid (DL-APV) (*10*), no MSCTs occurred in 21 10-s trials. In contrast, in untreated cultures 60 MSCTs were observed in 71 10-s trials. The effects of DL-APV were reversible: synaptically mediated $[Ca^{2+}]_i$ transients were observed after DL-APV was removed.

To ensure that the spatially restricted nature of the MSCTs was not due to the inability of some postsynaptic elements to exhibit elevations in $[Ca^{2+}]_i$, we also imaged these dendrites in the absence of TTX to monitor synaptic $[Ca^{2+}]_i$ transients (SCTs) produced by synchronous action

T. H. Murphy and J. M. Baraban, Department of Neuroscience, Johns Hopkins University School of Medicine, Baltimore, MD 21205.
W. G. Wier and L. A. Blatter, Department of Physiology, University of Maryland School of Medicine, Baltimore, MD 21201.

*To whom correspondence should be addressed.
†Present address: Department of Physiology, Loyola University Chicago, Maywood, IL 60153.